ELSEVIER

Journal of Molecular Catalysis A: Chemical 192 (2003) 153–170

JOURNAL OF MOLECULAR CATALYSIS A: CHEMICAL

www.elsevier.com/locate/molcata

Synthesis of ethyl β-naphthyl ether (neroline) using SO_4^{2-}/Al-MCM-41 mesoporous molecular sieves

M. Selvaraj [a,*], A. Pandurangan [a], K.S. Seshadri [b], P.K. Sinha [b], V. Krishnasamy [a], K.B. Lal [b]

[a] *Department of Chemistry, Anna University, Chennai 600025, India*
[b] *CWMF, BARC Facilities, Kalpakkam 603102, India*

Received 9 January 2002; accepted 8 July 2002

Abstract

The mesoporous molecular sieves Al-MCM-41 with Si/Al ratio equal to 30, was synthesized under hydrothermal conditions using cetyltrimethylammonium ($CTMA^+$) surfactants as template in the absence of auxiliary organics. The same ratio of Al-MCM-41 materials was impregnated using sulfuric acid, the materials such as sulfated Al-MCM-41 (SO_4^{2-}/Al-MCM-41). The mesoporous materials, viz. Al-MCM-41 and SO_4^{2-}/Al-MCM-41 were characterized using several techniques, e.g. inductively coupled plasma-atomic emission spectroscopy (ICP-AES), nephelometer, powder X-ray diffraction (XRD), Fourier transform-infra red spectroscopy (FT-IR), thermogravimetric–differential thermal analyzer (TG–DTA) and nitrogen adsorption measurements. ICP-AES studies indicated the content of Al in the mesoporous materials. Nephelometer studies indicated the SO_4^{2-} content in the SO_4^{2-}/Al-MCM-41. XRD studies indicated that the calcined materials of Al-MCM-41 and SO_4^{2-}/Al-MCM-41 had the standard MCM-41 structure. FT-IR studies indicated that Al ions were incorporated on the hexagonal mesoporous of Al-MCM-41 and sulfuric acid was impregnated into hexagonal Al-MCM-41 materials. Thermal stability of the as-synthesized Al-MCM-41 materials and SO_4^{2-}/Al-MCM-41 materials was studied using TG/DTA. The surface area, pore diameter, and pore volume of the mesoporous materials were calculated by BET and BJH equations, respectively. Crystallinity, surface area, pore diameter and pore volume of SO_4^{2-}/Al-MCM-41 decreased and expelling the aluminum from the Al-MCM-41 framework increased the Lewis acidity. The catalytic results were compared with those obtained by using sulfuric acid, amorphous silica-alumina, H-β, USY and H-ZSM-5 zeolites. The SO_4^{2-}/Al-MCM-41 catalysts was found to be more effective in the ethoxylation of hydroxyl biaromatics, for example, in the production of ethyl β-naphthyl ether (neroline) from β-naphthol using ethyl acetate as the ethoxylating reagent. The SO_4^{2-}/Al-MCM-41 catalyst exclusively forms the product of ethyl β-naphthyl ether and has much higher yields than other catalysts except USY.

Keywords: Al-MCM-41; SO_4^{2-}/Al-MCM-41; Ethoxylation of β-naphthol; Conversion of β-naphthol; Selectivity of ethyl β-naphthyl ether

1. Introduction

The recent syntheses of well-ordered mesoporous inorganic solids with pores of diameter 20–100 Å have opened a new field in advanced material research [1,2]. The mesoporous materials, the most studied of which is MCM-41, are prepared using surfactant

* Corresponding author. Tel.: +91-4114-480063; fax: +91-4114-480063.
E-mail address: selvarajman25@yahoo.com (M. Selvaraj).

1381-1169/02/$ – see front matter
PII: S1381-1169(02)00414-4

micelles (so-called liquid crystal templates), which act as structure directors for the product (synthesized) molecular sieves. Calcination burns off the organic template leaving behind a well-ordered inorganic framework with pores having diameter determined primarily by the size of the template surfactant molecules [3]. Stability of these mesoporous materials is an important factor when they are used as sorbents, solid catalysts, catalyst supports or ion exchangers [1,2]. Hydrothermal stability is of particular importance in any application involving the presence of water. In general, the hydrothermal stability (especially in boiling water) of pure silica MCM-41 material is very poor [4–6]. Indeed, when subjected to reactions in water for short periods of time, conventional pure silica MCM-41 materials are readily rendered amorphous [4]. The hydrothermal stability of pure silica MCM-41 materials can, however, be improved by adding various salts to their synthesized gel [6,7] or via post-synthesis modifications, which increase the pore wall thickness [8,9]. The incorporation of heteroatoms into the walls of MCM-41 has been reported to alter both the structural ordering and hydrothermal stability [10]. There is, therefore, considerable research interest in the hydrothermal stability of heteroatom containing mesoporous silica, and in particular in Al-containing MCM-41 materials, which exhibit ion exchange and solid acid catalytic activity.

Corma et al. [11] first reported the details of synthesis and characterization of aluminum incorporated mesoporous materials. However, the catalytic activity of the material was low in comparison to the usual silica-alumina catalyst and also the thermal stability was poor. Van Hooff and co-workers [12] also reported synthesis and characterization of the Al-MCM-41, wherein incorporation of an excess of aluminum formed an impure crystal-phase tridimite, and the Lewis acid site prevailed because of the octahedral non-framework aluminum, accompanied with the collapse of the structure.

β-Naphthyl methyl ether has been used in perfumery; it is traditionally manufactured from β-naphthol and methanol in the presence sulfuric acid. However, the drawbacks of such a process include corrosion, safety hazards, separation procedures and environmental problems due to sulfuric acid. Therefore, the authors attempted to utilize solid acid catalysts to prepare β-naphthyl methyl ether. Particularly, Chen et al. [13] first reported the details of the synthesis and characterization of sulfuric acid impregnated mesoporous materials. He synthesized β-naphthyl methyl ether using SO_4^{2-}/Al-MCM-41. The catalytic activity of SO_4^{2-}/Al-MCM-41 for the synthesis of β-naphthyl methyl ether was high in comparison to the sulfuric acid, amorphous silica-alumina, γ-alumina and H-ZSM-5 zeolites except USY.

Ethyl β-naphthyl ether has been synthesized using β-naphthol and ethyl acetate in the presence of sulfuric acid by Patai and Bentev [14]. Ethyl β-naphthyl ether (neroline) has also been used in perfumery; it is conventionally synthesized from β-naphthol and ethyl acetate in the presence of strong acid as catalyst. However, the drawbacks of such a process include corrosion, safety hazards, separation procedure, and environmental problems due to the use of strong acid. Therefore, our present study includes the preparation and the characterization of Al-MCM-41 with aluminum isopropoxide under hydrothermal conditions. The synthesized Al-MCM-41 materials were modified with sulfuric acid and the resulting materials are known as sulfated Al-MCM-41 (SO_4^{2-}/Al-MCM-41) materials. These materials have been used as catalyst in the synthesis of ethyl β-naphthyl ether. The catalytic reaction was carried out under various conditions, viz. reaction temperature, reaction time and ethyl acetate/β-naphthol using SO_4^{2-}/Al-MCM-41 as catalyst. These catalytic results are correlated and compared with those of sulfuric acid (68.9 mol%) and other solid acid catalysts, such as Al-MCM-41, amorphous silica-alumina, H-β, USY and H-ZSM-5 zeolite.

2. Experimental

2.1. Materials

The syntheses of Al-MCM-41 and SO_4^{2-}/Al-MCM-41 materials were carried out by hydrothermal and impregnation methods, respectively, and using tetraethylorthosilicate (TEOS), cetyltrimethylammonium bromide ($C_{16}H_{33}(CH_3)_3N^+Br$), tetraethylammonium hydroxide ($(C_2H_5)_4NOH$), sulfuric acid (H_2SO_4). The synthesis of ethyl β-naphthyl ether was carried out by liquid phase reaction using 2-naphathol ($C_{12}H_{12}O$), ethyl acetate ($CH_3CO_2C_2H_5$) and ethanol

(C_2H_5OH). The chemicals used were of AR grade purchased from Aldrich.

2.2. Commercial catalytic materials

Amorphous silica-alumina (Si/Al = 5.7, Strem), H-β (Strem), USY (Si/Al = 27.5, PQ) and H-ZSM-5 (S/Al = 25.5, PQ) were obtained from commercial sources. These catalysts were calcined at 500 °C for 6 h before catalytic reaction.

2.3. Synthesis of Al-MCM-41 and SO_4^{2-}/Al-MCM-41

2.3.1. Synthesis of Al-MCM-41

For the synthesis of the Al-MCM-41 (Si/Al = 30) material, 22.3 ml (1 mol) of tetraethylorthosilicate was mixed with 0.68 g (0.033 mol) of aluminum isopropoxide (dissolved in 5 ml of deionized water). The mixture solution was stirred for 30 min at a speed of about 250 rpm and tetraethylammonium hydroxide solution (10% water) was added with continuous stirring for another 30 min at a speed of about 250 rpm until the gel formation (pH = 11). After that, 7.2 g (0.2 mol) of cetyltrimethylammonium bromide was added drop by drop (30 ml/h) through the dual syringe pump so that the gel was changed into suspension. The suspension was transferred into teflon-lined steel autoclave and heated to 150 °C for 48 h. After cooling to room temperature, the material was recovered by filtration, washed with deionized water and ethanol, dried in air at 100 °C for 1 h and finally calcined in flowing air at 540 °C for 6 h. The synthesis procedure is shown in Fig. 1.

2.3.2. Synthesis of SO_4^{2-}/Al-MCM-41

The sulfated Al-MCM-41 (SO_4^{2-}/Al-MCM-41) was prepared by impregnating an amount of 50 ml

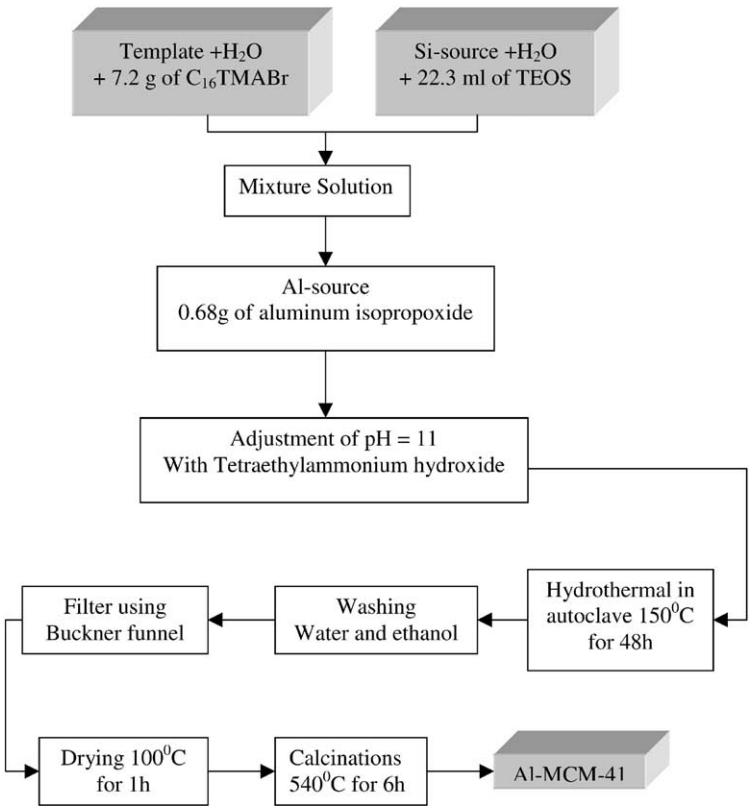

Fig. 1. Flow chart of the synthesis of Al-MCM-41.

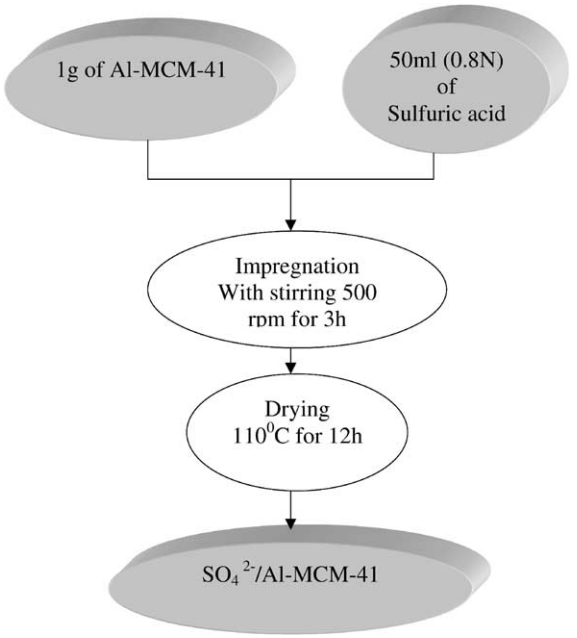

Fig. 2. Flow chart of the synthesis of SO_4^{2-}/Al-MCM-41.

(0.8 N) of sulfuric acid on 1 g of Al-MCM-41 with stirring 500 rpm for 3 h. Then the sample was dried at 110 °C for 12 h. Sulfuric acid impregnation procedure is shown in Fig. 2.

2.4. Characterization

The Al content in SO_4^{2-}/Al-MCM-41 and Al-MCM-41 was recorded using ICP-AES with Allied Analytical ICAP 9000. The SO_4^{2-} content in SO_4^{2-}/Al-MCM-41 with barium chloride was recorded using nephelometer with CL52D (Elico Limited, India).

The crystalline phase identification and phase purity determination of the calcined samples of Al-MCM-41 (Si/Al = 30) and sulfated impregnated Al-MCM-41 in the same molar ratio of Si/Al = 30 were carried out by X-ray diffraction (XRD, Philips, Holland) using nickel filtered Cu Kα radiation (λ = 1.5406 Å). The samples were scanned from 0.5 to 5° (2θ) angle in steps of 0.5°, with a count of 5 s at each point. In order to protect the detector from the high energy of the incident and diffracted beam, slits were used in this work.

Infra red spectra were recorded with a Nicolet Impact 410 Fourier transform-infra red (FT-IR) spectrometer in KBr pellet (0.005 g sample with 0.1 g KBr) scan number 36, resolution 2 cm^{-1}. The data was treated with Omnic Software.

Thermogravimetric–differential thermal analysis (TG–DTA) was carried out in Rheometric Scientific ($STAH^+$) thermobalance. A total of 10–15 milligrams of the as-synthesized samples Al-MCM-41 and SO_4^{2-}/Al-MCM-41 were loaded, and the airflow used was 50 ml/min. The heating rate was 20 K/min and the final temperature was 1000 °C.

N_2-adsorption isotherms were measured at −197 °C using a Micromeritics ASAP 2000. Prior to the experiments, the samples were dehydrated at 350 °C until the vacuum pressure was below 8 mmHg. The surface area was calculated using the BET method based on adsorption data in the partial pressure (P/P_0) range 0.0–0.1 and the pore diameter and pore volume were determined from the amount of N_2 adsorbed at a $P/P_0 = 1$ using BJH method.

2.5. Experimental for synthesis of ethyl β-naphthyl ether

2.5.1. Catalytic reaction

The catalyst (0.5 g) was added into a mixture of ethyl acetate and β-naphthol (various molar ratio), and the reaction was carried out in a stirred batch autoclave reactor (100 ml, Autoclave Engineers) at reaction temperatures, viz. 80, 160 and 210 °C for different reaction time (h). The reaction products were recovered from the reactor after cooling to 0 °C.

2.5.2. Analysis of reaction products

After reaction, the catalyst solution was centrifuged and the supernatant was collected. This was followed by addition of ethanol to the catalyst and was centrifuged and the supernatant was collected. This was repeated twice. To this, again ethanol was added and the centrifuge tube tightly sealed and magnetically stirred at 40 °C for 1 h. This step was carried out to recover the catalyst if it was left in the solution. This step was repeated two or three times. The supernatant solutions collected in the above steps were maintained at 0 °C for 1 h. After 1 h, the lustrous crystal formed in both solutions were heated to (>38 °C) and maintained at this temperature for 1 h. The clear solutions

were analyzed with a GC (HP 5890 Series II) using a flame-ionization detector and a 50 m × 0.2 mm PONA column (Supelco).

2.6. Experiment on leaching of sulfate from SO_4^{2-}/Al-MCM-41

After the catalyst reaction, the appropriate amount of catalyst was equilibrated with distilled water, and kept in water bath and the supernatant was checked for SO_4^{2-} using barium chloride. The above experiment was performed in duplicate.

3. Results and discussion

3.1. Yield of synthesis

The mass of the as-synthesized Al-MCM-41 (Si/Al = 30) was found to be 10.2 g, which reduced to 6.3 g on calcination. The mass value for the SO_4^{2-}/Al-MCM-41 was 8.2 g. The Al content in both catalysts was found to be 0.9 g containing Si/Al = 30 using ICP-AES. The SO_4^{2-} was found to be 1960 ppm in the SO_4^{2-}/Al-MCM-41 using nephelometer.

3.2. XRD

Fig. 3 shows the powder X-ray diffraction patterns of calcined Al-MCM-41 materials. The X-ray diffractograms of the Al-MCM-41 and SO_4^{2-}/Al-MCM-41 materials, after calcination in air at 540 °C for 6 h, contain, in addition to sharp d_{100} reflection line near $2\theta = 1.93°$, broad peaks near $2\theta = 3.33°$ (1 1 0) and 3.83° (2 0 0). The SO_4^{2-}/Al-MCM-41 material after getting dried at 110 °C for 12 h, contain, in addition to the sharp d_{100} reflection line near $2\theta = 2.0°$, broad peaks near $2\theta = 3.48°$ (1 1 0) and 3.98° (2 0 0). The broadening effects of higher reflection lines can be due to small crystallites [15]. Physicochemical properties of these mesoporous materials are summarized in Table 1. Table 1 illustrates that the pore-to-pore distance of Al-MCM-41 could be determined by the XRD patterns. The XRD patterns of calcined Al-MCM-41 with characteristic peaks of hexagonal symmetry and with d_{100} of 45.73 Å are shown in Fig. 3a.

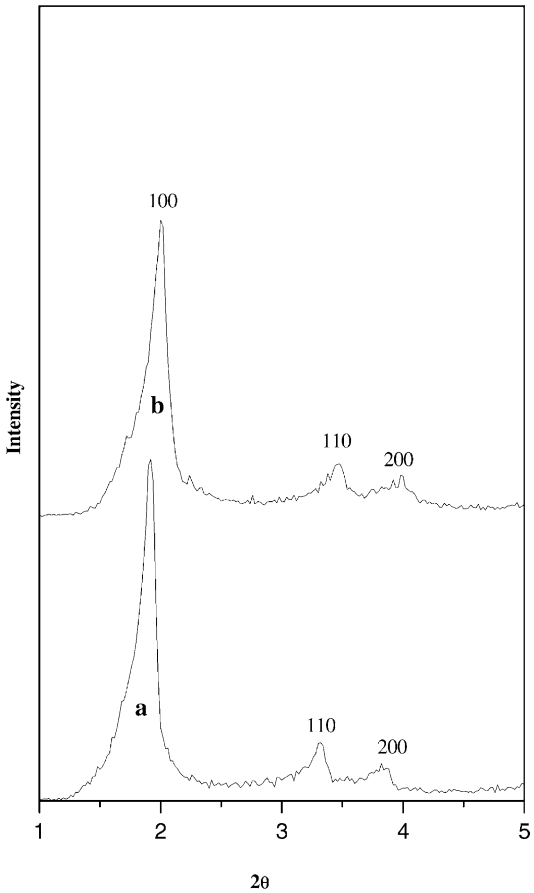

Fig. 3. XRD powder patterns of (a) calcined Al-MCM-41, and (b) SO_4^{2-}/Al-MCM-41.

Table 1
Physicochemical characterization of Al-MCM-41 and SO_4^{2-}/Al-MCM-41

Samples	*d*-Spacing value (Å)	Unit cell parameter (Å)	BET surface area (m^2/g)	Pore diameter (Å)	Pore volume (cm^3/g)
Al-MCM-41	45.7	52.8	1099	28.3	1.48
SO_4^{2-}/Al-MCM-41	44.1	50.92	698	25.8	0.84

The repeating distance (a_0) between pore centers was 52.8 Å. The hexagonal unit cell parameter (a_0) was calculated using $2d_{100}/3$ from d_{100}, which was obtained from the peak in the XRD pattern by Bragg's equation ($2d \sin\theta = \lambda$, where $\lambda = 1.5406$ Å for the Cu Kα line). The value of a_0 was equal to the internal pore diameter plus one pore wall thickness. In general, at the synthesis condition used, the crystallization reaction is non-stoichiometric and the crystal's Si/Al ratio is always greater than in the hydrogel containing aluminum [16]. Incorporation of aluminum into the silicate framework the size of the unit cell decreases when the source of Al is Al-isopropoxide, and then in general as Al content increases, unit cell parameter decreases. The data obtained for the calcined materials are in good agreement with those reported by Beck et al. [17]. Excess incorporation of aluminum (low Si/Al ratio) might lead to the collapse of the structure, as reported by Kin et al. [18] for Al-MCM-41 (Si/Al = 10) prepared at a pH of 11. Impregnation of Al-MCM-41 with sulfuric acid results in the decrease of crystallinity, *d*-spacing value and unit cell parameter than that of Al-MCM-41 [13].

3.2.1. Adsorption isotherm of nitrogen

Fig. 4a and b show the isotherm of nitrogen adsorption on the calcined Al-MCM-41 and SO_4^{2-}/Al-MCM-41 measured at liquid nitrogen temperature (−197 °C). Three well-defined stages may be identified: (1) a slow increase in nitrogen uptake at low relative pressure corresponding to monolayer–multilayer adsorption on the pore walls; (2) a sharp step at intermediate relative pressures indicative of capillary condensation within mesopores; (3) a plateau with a slight inclination at high relative pressures associated with multiplayer adsorption on the external surface of the crystals [19]. The fourth stage, characterized by a sharp rise in N_2 uptake as the pressure reaches saturation ($P/P_0 = 1$), may be identified in some isotherms. Mesoporous materials with high Al content generally raise the isotherm lines at high pressure, which is attributed to the condensation of nitrogen within voids formed by crystal aggregates.

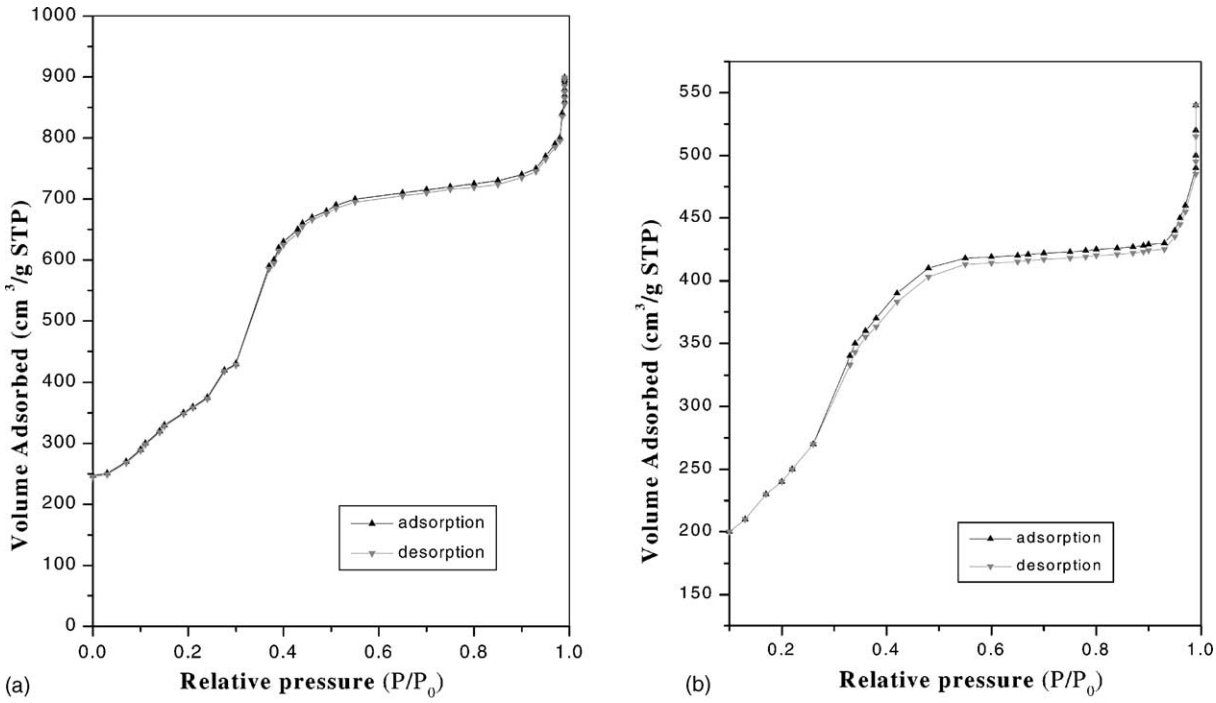

Fig. 4. (a) N_2-adsorption isotherms of calcined Al-MCM-41; (b) N_2-adsorption isotherms of SO_4^{2-}/Al-MCM-41.

It is worthwhile to note that the sharpness and height of the capillary condensation (pore filling) step in the isotherms is a measure of the pore size uniformity. Departures from a sharp and clearly defined pore-filling step are usually an indication of increase in pore size heterogeneity (i.e. widening of pore size distribution). The samples exhibit isotherms with a well-developed step in the relative pressure (P/P_0) range corresponding from 0.3 to 0.36 for Al-MCM-41 and from 0.26 to 0.32 for SO_4^{2-}/Al-MCM-41. A characteristic hysteresis loop observed for both samples in the region of P/P_0 above 0.4 is assigned to the capillary condensation in the mesopores [19]. However, the capillary condensation step is much higher and steep for the Al-MCM-41 than that for the SO_4^{2-}/Al-MCM-41. In general, the isotherms indicate that all of the samples possess good mesopore structural ordering and a narrow pore size distribution and any structural changes resulting from Al incorporation are not necessarily at the expense of pore uniformity. The surface area, pore diameter and pore volume are given in Table 1. The pore diameter of Al-MCM-41 is higher than that of SO_4^{2-}/Al-MCM-41 due to the presence of textural mesoporosity [20]. Sulfuric acid treatment of Al-MCM-41 sample results in a decrease of surface area from 1099 to 698 m^2/g that is consistent by lower relative pressure (P/P_0). Thus, the surface area, pore diameter and pore volume of SO_4^{2-}/Al-MCM-41 material is lower than that of Al-MCM-41 material and the sulfation of Al-MCM-41 results in a decrease of the pore volume from 1.48 to 0.84 cm^3/g. (Since the Kelvin equation is not valid for pores below 18 Å, the BJH approach can only be used for mesoporous material.)

3.2.2. FT-IR spectroscopy

Infra red spectroscopy had been used extensively for the characterization of transition-metal cation modified zeolites. In the FT-IR spectrum of calcined siliceous MCM-41, the asymmetric and symmetric stretching vibration bands of framework Si–O–Si bands, assigned by Sohn et al. [21] for zeolites, appeared at 1123 and 814 cm^{-1}. In the as-synthesized Al-MCM-41, the IR spectrum was measured in 400–4000 cm^{-1} range in a few steps during sample preparation and is shown in Fig. 5a. The as-synthesized sample exhibits absorption bands around 2921 and 2851 cm^{-1} corresponding to *n*-C–H and *d*-C–H vibrations of the surfactant molecules. The broad bands around 3500 cm^{-1} may be attributed surface silanols and adsorbed water molecules, while deformational vibrations of adsorbed molecules cause the adsorption bands at 1623–1640 cm^{-1} [22]. The absorption band at 1069 and 1223 cm^{-1} are due to asymmetric stretching vibrations of Si–O–Si bridges, but in the opposite direction are observed for the 962 cm^{-1} bands due to Si–O–Al vibrations in aluminum incorporation of silanols. When various metals are incorporated, the intensity of this band increases. This is generally considered to be a proof of the incorporation of the heteroatom into the framework. Cambler et al. [23] have reported similar stretching vibrations of Si–OH groups present at defect sites. Disappearance of bands at 2851 and 2921 cm^{-1}, can be concluded that calcination of the original framework were completed and indicate the absence of organic molecule, which

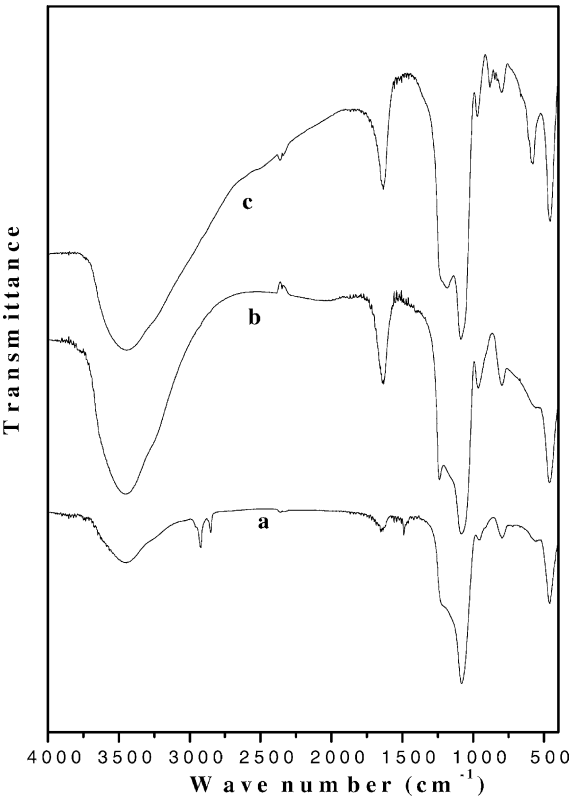

Fig. 5. FT-IR adsorption spectra of (a) as-synthesized Al-MCM-41, (b) calcined Al-MCM-41, and (c) SO_4^{2-}/Al-MCM-41.

completely disappeared from the calcined Al-MCM-41. The vibration bands of calcined Al-MCM-41 can be shifted from 1 to 3 or 5 cm^{-1}, except the vibration bands of 2921 and 2821 cm^{-1} due to removal of organic molecules after calcinations. An FT-IR spectrum of calcined Al-MCM-41 is shown in Fig. 5b. Upon introduction of Al, for most of the bands SO_4^{2-} shifted to higher wave numbers, consistent with their incorporation in lattice positions. Additionally, an absorption band of 963 cm^{-1} assigned to a stretching vibration of Si–O–Al linkage was observed.

In the SO_4^{2-}/Al-MCM-41, the IR spectrum was measured in 400–4000 cm^{-1} range in a few steps during sample preparation and is shown Fig. 5c. The sulfated sample exhibits absorption bands around 3500 cm^{-1}, which may be attributed to surface silanol groups and adsorbed water molecules [22]. The absorption bands at 1186, 876 and 585 cm^{-1} are due to strong stretching vibrations of HSO_4^- [24]. The above results from the FT-IR analysis (Fig. 5c) results carried out for sulfate impregnated Al-MCM-41 in particular for the absorption of sulfate is similar to the FT-IR analysis carried out by Rao for sulfate impregnated aluminosilicate. The SO_2 deformation frequency has been assigned in the region 876 and 585 cm^{-1}. The absorption bands at 1186 cm^{-1} is due to symmetric vibrations of S–O–Si bridges, but in the opposite direction are observed for the 963 cm^{-1} bands due to Si–O–Al vibrations in aluminum incorporated silanols. The absorption band at 799 cm^{-1} is due to the symmetric Si–O stretching vibration and band at 876 cm^{-1} is due to the symmetric S–O stretching vibrations.

3.2.3. Thermal analysis

Thermogravimetric analysis [5] of the crystals shows distinct weight losses that depend, on the framework composition (Table 2). Representative thermograms are given in Fig. 6. The minor weight loss below 150 °C corresponds to the desorption of physisorbed water (or ethanol) in the voids formed by crystal agglomeration. Weight losses in the temperature range 150–350 °C are attributed to the decomposition and removal of occluded organics. Weight losses in this temperature range are not as large as in the parent silicate because of stronger sorbate–sorbent interactions at the aluminosilicate surface. In the temperature range 280–340 °C, the oxidative decomposition of residual organic compounds occurs which is accompanied by exotherms whose number and intensity depends on the aluminum content of the crystal. The 350–550 °C was the region of surfactant associated with Al–O. There was almost no exothermal peak after 550 °C, which indicated the surfactant, had been removed completely. In other words, it could show that the Al-MCM-41 material structure was quite stable because of the straight weight loss line after 550 °C. The total weight loss at 1000 °C of the Al-MCM-41 sample is in 44.11, without any clear dependence on the Si/Al ratio or aluminum source of the sample. However, the distribution of successive weight losses depends on the framework Si/Al ratio.

Representative thermograms are given in Fig. 6. The major exothermic reaction peak is assigned the minor weight loss below 150 °C corresponds to the desorption of physisorbed water in the voids formed by crystal agglomeration and also the minor exothermic peak occurring at the 150–350 °C is attributed to the decomposition of SO_4^{2-} into SO_2 gas. Thus, the total weight loss at 1000 °C of the SO_4^{2-}/Al-MCM-41 sample is in the 67.51%, without any clear dependence on the sulfate ion containing aluminum source of the sample.

3.2.4. Ethoxylation of β-naphthol

Ethyl β-naphthyl ether has been synthesized by Patai and Bentev [14], when it is traditionally manufactured from β-naphthol and ethyl acetate in the

Table 2
Thermogravimetric results (in air) for the SO_4^{2-}/Al-MCM-41 and Al-MCM-41

Samples	Weight loss (wt.%)			
	50–150 °C	150–350 °C	350–550 °C	Total
Al-MCM-41	4.10	34.21	5.80	44.11
SO_4^{2-}/Al-MCM-41	45.21	22.3	–	67.51

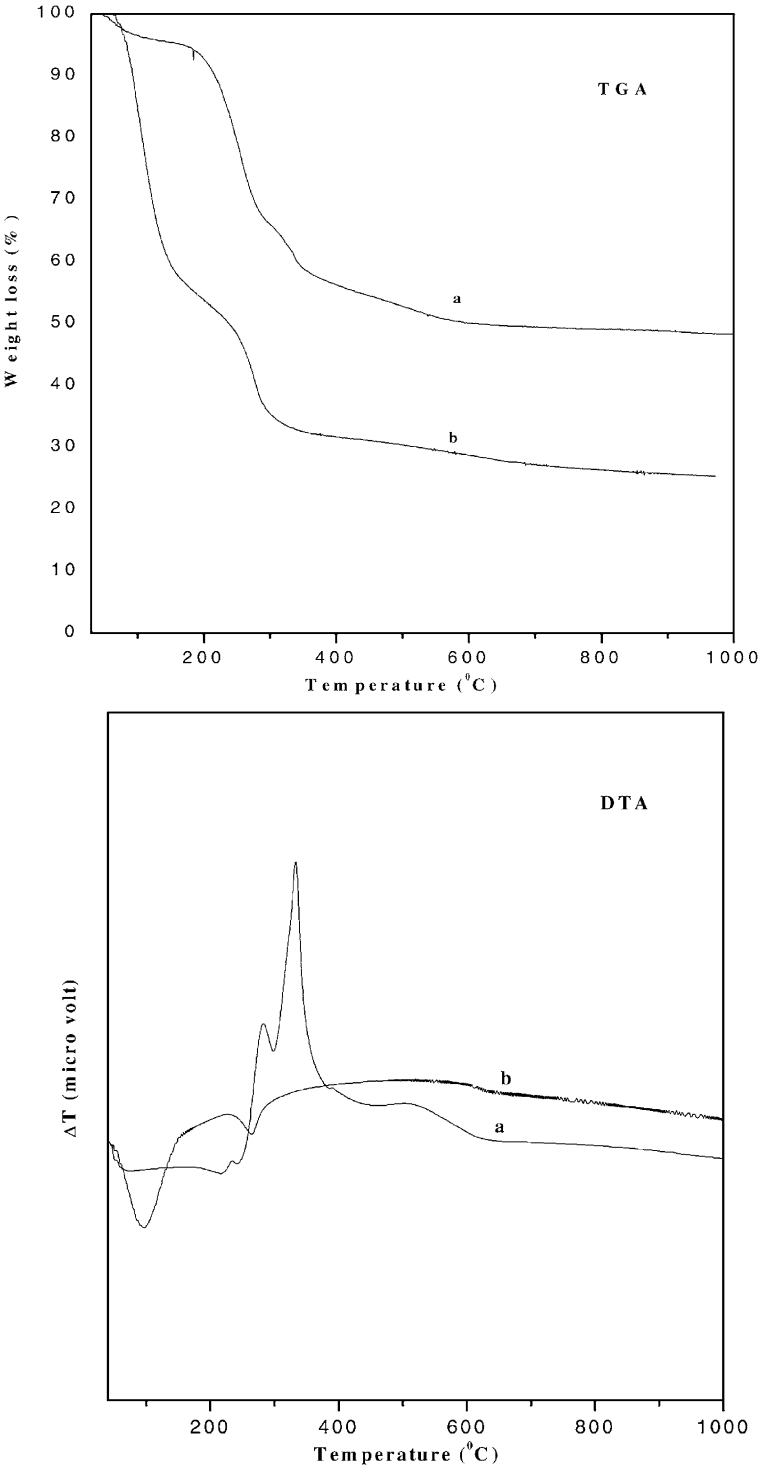

Fig. 6. TG/DTA plots of (a) as-synthesized Al-MCM-41, and (b) SO_4^{2-}/Al-MCM-41.

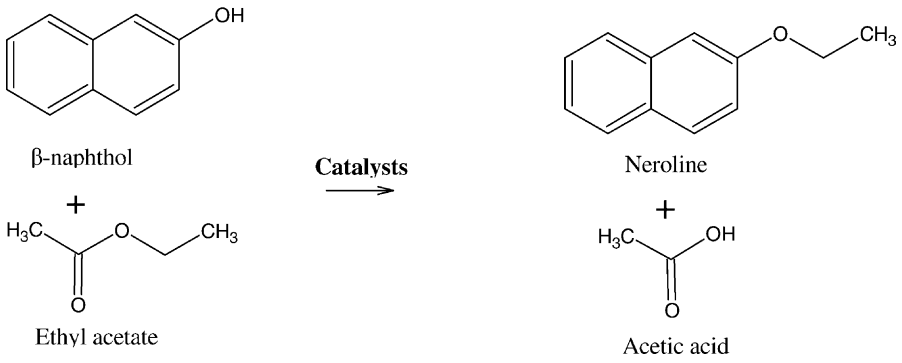

Fig. 7. Reaction scheme in the ethoxylation of β-naphthol with ethyl acetate.

strong acid as catalyst; the drawbacks of such a process include corrosion, safety hazards, separation procedures and environmental problem due to the use of strong acid. So, we have synthesized ethyl β-naphthyl ether using β-naphthol and ethyl acetate as ethoxylating reagent in the presence of SO_4^{2-}/Al-MCM-41. It is synthesized by varying the preparative parameters and the effects, viz. reaction time, reaction temperature and ethyl acetate/β-naphthol molar ratio are discussed below. The catalytic activity of SO_4^{2-}/Al-MCM-41 is compared to different catalysts and those results are given below. The ethoxylation of β-naphthol reaction is shown in the Fig. 7.

3.2.4.1. Yield of ethyl β-naphthyl ether. When the reaction of ethoxylation of β-naphthol was carried out in the presence of SO_4^{2-}/Al-MCM-41, the conversion of β-naphthol was 70.3% and selectivity was 98.4%. Hence, all the subsequent experiments were carried out only with SO_4^{2-}/Al-MCM-41 catalyst, it was compared with various catalysts with respect to the yield of ethyl β-naphthyl ether, which resulted into higher yield except USY.

In our experiments, it was observed that the yield of ethyl β-naphthyl ether was higher than that of acetic acid. The mechanism proposed by Patai and Bentev [14] for the formation of ethyl β-naphthyl ether from β-naphthol and ethyl acetate in strong acid medium involves the ethoxylation of β-naphthol using ethyl acetate followed by removal of acetic acid. This reaction is expected to be mediated through an ethyl carbocation. The active carbocation as electrophile will attack the lone pair of electron available as the oxygen of the β-naphthol followed by removal of hydroxyl ion of proton from β-naphthol with the formation β-naphthyl ether. In the present studies, we used the solid acid catalyst, SO_4^{2-}/Al-MCM-41 in place of sulfuric acid and the results are reported.

The rate of alkylation depends upon the pore structure and acidity behavior of the catalyst. The acid sites of SO_4^{2-}/Al-MCM-41 and Al-MCM-41 are reported by Chen et al. [13]. It was reported that the acid site of SO_4^{2-}/Al-MCM-41 are higher than that Al-MCM-41. Hence the yield of the final product ethyl β-naphthyl ether depends on the rate of ethoxylation, which in turn depends on the substrate and catalyst features (pore structure and acidity). This observation indicates that the number of Lewis acid sites in SO_4^{2-}/Al-MCM-41 is higher than that in Al-MCM-41; as hydrogen ion concentration is higher in SO_4^{2-}/Al-MCM-41 than that in Al-MCM-41. Thus, the formation of ethyl β-naphthyl ether is higher in SO_4^{2-}/Al-MCM-41 than that in Al-MCM-41.

3.2.4.2. Variation with ethyl acetate/β-naphthol molar ratio. Ethoxylation of β-naphthol was carried out at 5:1–20:2 molar ratios for SO_4^{2-}/Al-MCM-41 catalyst at 80, 160 and 210 °C for 60 min and are summarized in Table 3. β-Naphthol conversion and selectivity of ethyl β-naphthyl ether are 70.3 and 98.4%, respectively, in the molar ratio of 10:1. By the reaction property, 1 mol of β-naphthol has been neutralized by 10 mol of ethyl acetate, the conversion of β-naphthol and selectivity of ethyl β-naphthyl ether are higher than other molar ratios. But, the conversion of β-naphthol and the selectivity of ethyl

Table 3
Ethoxylation of β-naphthol: variation with ethyl acetate/β-naphthol molar ratio

Reaction temperature (°C)	Ethyl acetate/β-naphthol molar ratio	β-naphthol conversion (mol%)	Selectivity (mol%)	
			Ethyl β-naphthyl ether	Acetic acid
80	5:1	7.32	45.8	54.2
	10:1	35.65	69.3	30.7
	15:1	33.22	65.7	34.3
	20:1	30.12	58.3	41.7
	15:2	28.30	48.2	51.8
	20:2	20.50	43.2	56.8
160	5:1	17.3	53.2	46.8
	10:1	70.3	98.4	1.6
	15:1	68.3	88.3	11.7
	20:1	64.7	81.2	18.8
	15:2	50.2	68.3	31.7
	20:2	49.3	58.3	41.7
210	5:1	13.2	48.1	51.9
	10:1	58.2	90.2	9.8
	15:1	45.3	81.1	18.9
	20:1	41.2	73.2	26.8
	15:2	38.3	68.3	31.7
	20:2	30.2	62.3	37.7

Reaction conditions: 0.5 g of catalyst; reaction time, 1 h; 1000 rpm (speed stirring).

β-naphthyl ether are low in the other molar ratio because the reactants have not been neutralized within them (ethyl acetate/β-naphthol). Further, the highest conversion of β-naphthol (%) and selectivity of ethyl β-naphthyl ether (%) were obtained at ethyl acetate: β-naphthol ratio of 10:1 as can be seen in Figs. 8 and 9, respectively. Thus, the conversion of β-naphthol and the selectivity of ethyl β-naphthyl ether are

Table 4
Ethoxylation of β-naphthol: variation with reaction time (min)

Reaction temperature (°C)	Reaction time (min)	β-Naphthol conversion (mol%)	Selectivity (mol%)	
			Ethyl β-naphthyl ether	Acetic acid
80	30	25.21	50.30	49.70
	60	35.65	69.30	30.70
	90	34.32	60.21	39.79
	120	33.21	55.30	44.70
	150	30.21	30.30	69.70
160	30	50.45	75.30	24.70
	60	70.30	98.4	1.60
	90	65.3	94.3	5.70
	120	51.3	88.3	11.70
	150	48.3	70.3	29.70
210	30	43.1	67.3	32.7
	60	58.2	90.2	9.8
	90	43.2	67.3	32.7
	120	38.1	57.3	42.7
	150	23.2	47.3	52.7

Reaction conditions: 0.5 g of catalyst; ethyl acetate/β-naphthol molar ratio; 1000 rpm (speed stirring).

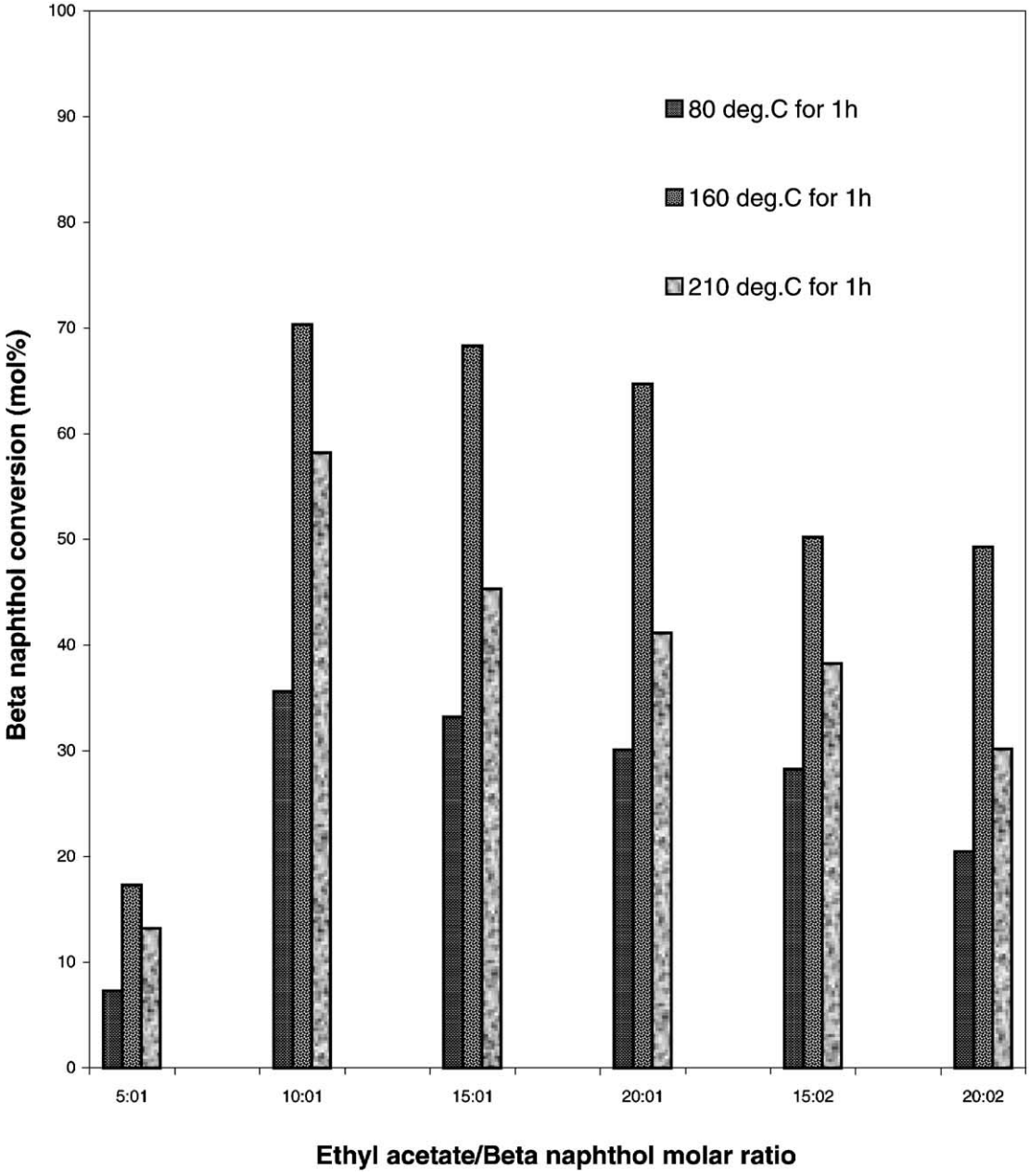

Fig. 8. Variation of conversion of β-naphthol (mol%) with ethyl acetate/β-naphthol molar ratio.

higher in the 10:1 molar ratio than that other molar ratio.

3.2.4.3. Variation with reaction time. Ethoxylation of β-naphthol was carried out at 30–150 min for SO_4^{2-}/Al-MCM-41 catalysts at 10:1 molar ratio. The results of variation of conversion of β-naphthol (%) and selectivity of ethyl β-naphthyl ether with different reaction time and temperature are presented in Table 4. As the reaction time increased, the

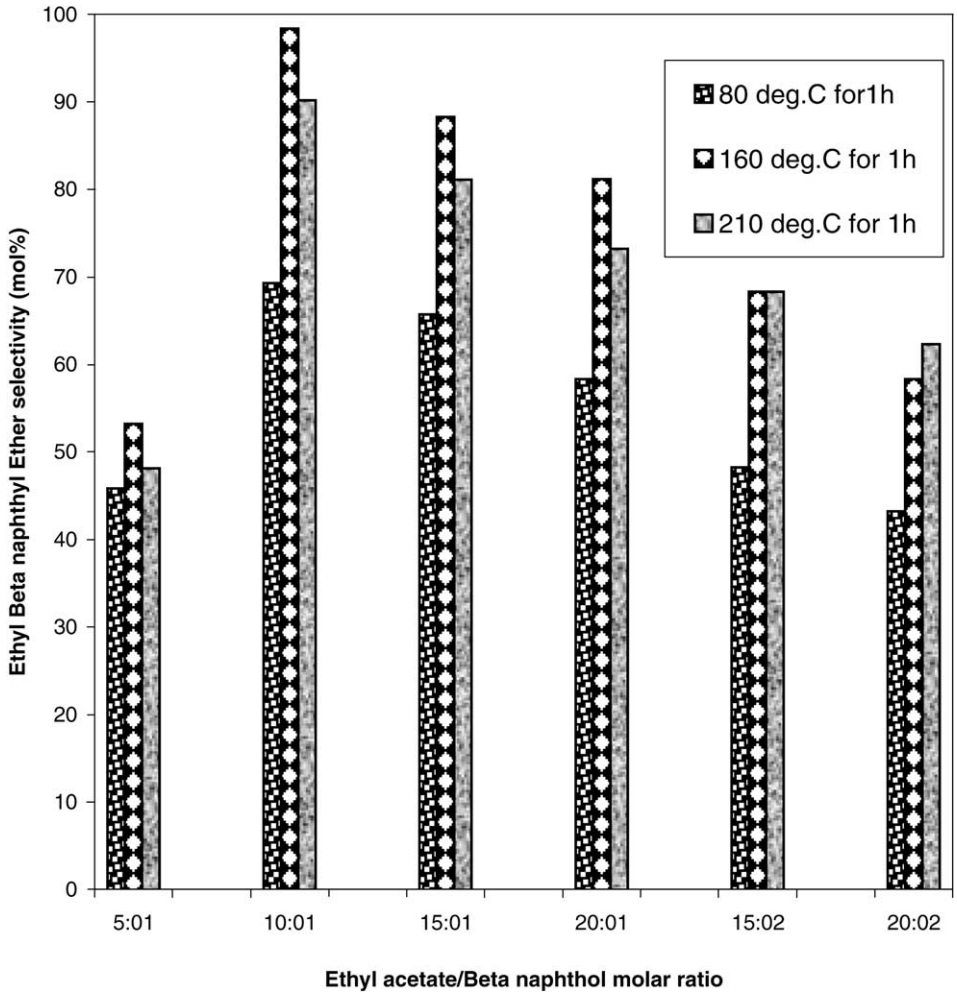

Fig. 9. Variation of ethyl β-naphthyl ether selectivity with ethyl acetate/β-naphthol molar ratio.

conversion of β-naphthol (%) and the selectivity of ethyl β-naphthyl ether also decreased in the latter. These may be due to the deactivation of the catalyst by the formation of coking and decrease in the activity of active sites of catalyst. The variation of conversion of β-naphthol (%) and selectivity of ethyl β-naphthyl ether (%) with different reaction time are presented in Figs. 10 and 11, respectively.

3.2.4.4. Effect of zelolites and Al-MCM-41 as catalysts. Both the catalytic activity and the yield of ethyl β-naphthyl ether follow the decreasing order: SO_4^{2-}/Al-MCM-41 ≈ USY > H_2SO_4 > H-β > Al-MCM-41 > Silica–alumina > H-ZSM-5 and the catalytic results in Table 5. Based on the results from FT-IR of adsorbed pyridine, TPD of the ammonia and those reported elsewhere [25], the catalyst acid strength also exhibits a similar trend, except H-ZSM-5 zeolite. As the ethoxylation of β-naphthol is an acid-catalyzed reaction, the conversion of β-naphthol is correlated to the catalyst acid strength and the conversion of β-naphthol with various catalysts was shown in Fig. 12. Although

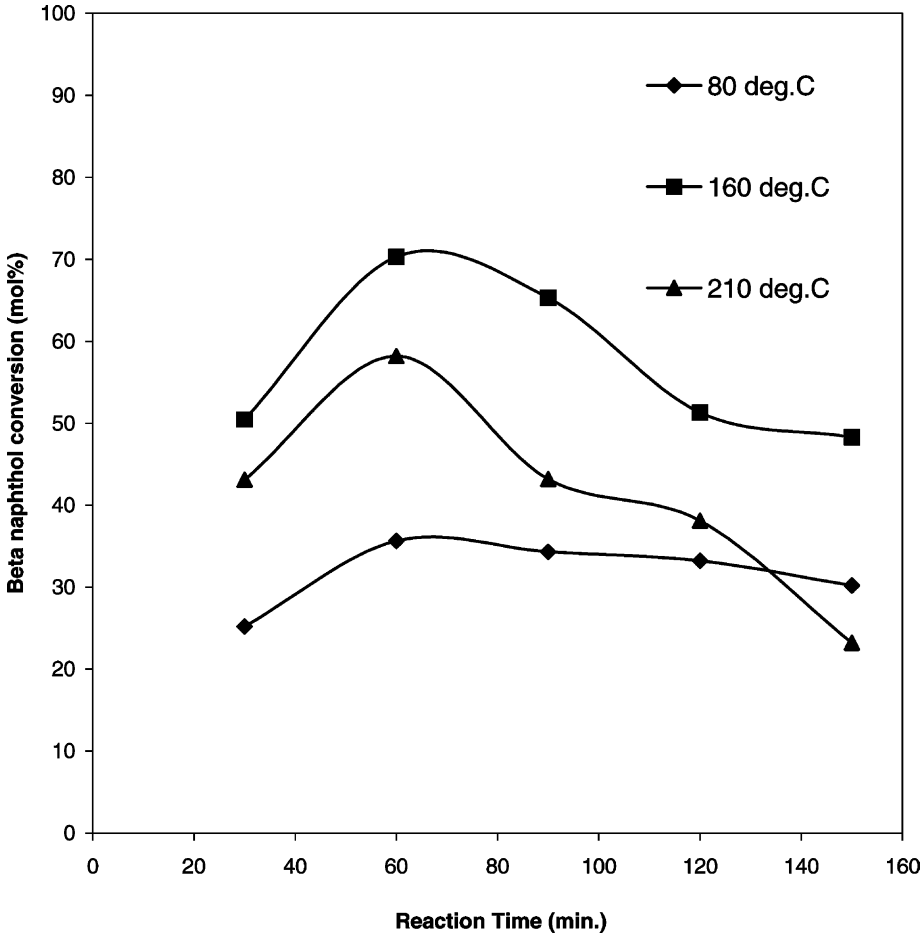

Fig. 10. Variation of conversion of β-naphthol (mol%) with reaction time (min).

Table 5
Ethoxylation of β-naphthol: variation with different catalysts

Number	Different catalyst (0.5 g)	β-Naphthol conversion (mol%)	Selectivity (mol%)	
			Ethyl β-naphthyl ether	Acetic acid
1	SO_4^{2-}/Al-MCM-41	70.3	98.4	1.6
2	Al-MCM-41	40.8	88.3	11.7
3	USY	70.0	98.4	1.6
4	H-β	60.36	76.4	23.6
5	H-ZSM-5	7.23	65.0	35.0
6	Silica-alumina	21.31	68.5	31.5
7	H_2SO_4	68.90	78.4	21.6

Reaction conditions: 0.5 g of catalyst; reaction temperature, 160 °C; reaction time, 1 h; 1000 rpm (speed stirring); ethyl acetate/β-naphthol mole ratio = 10:1.

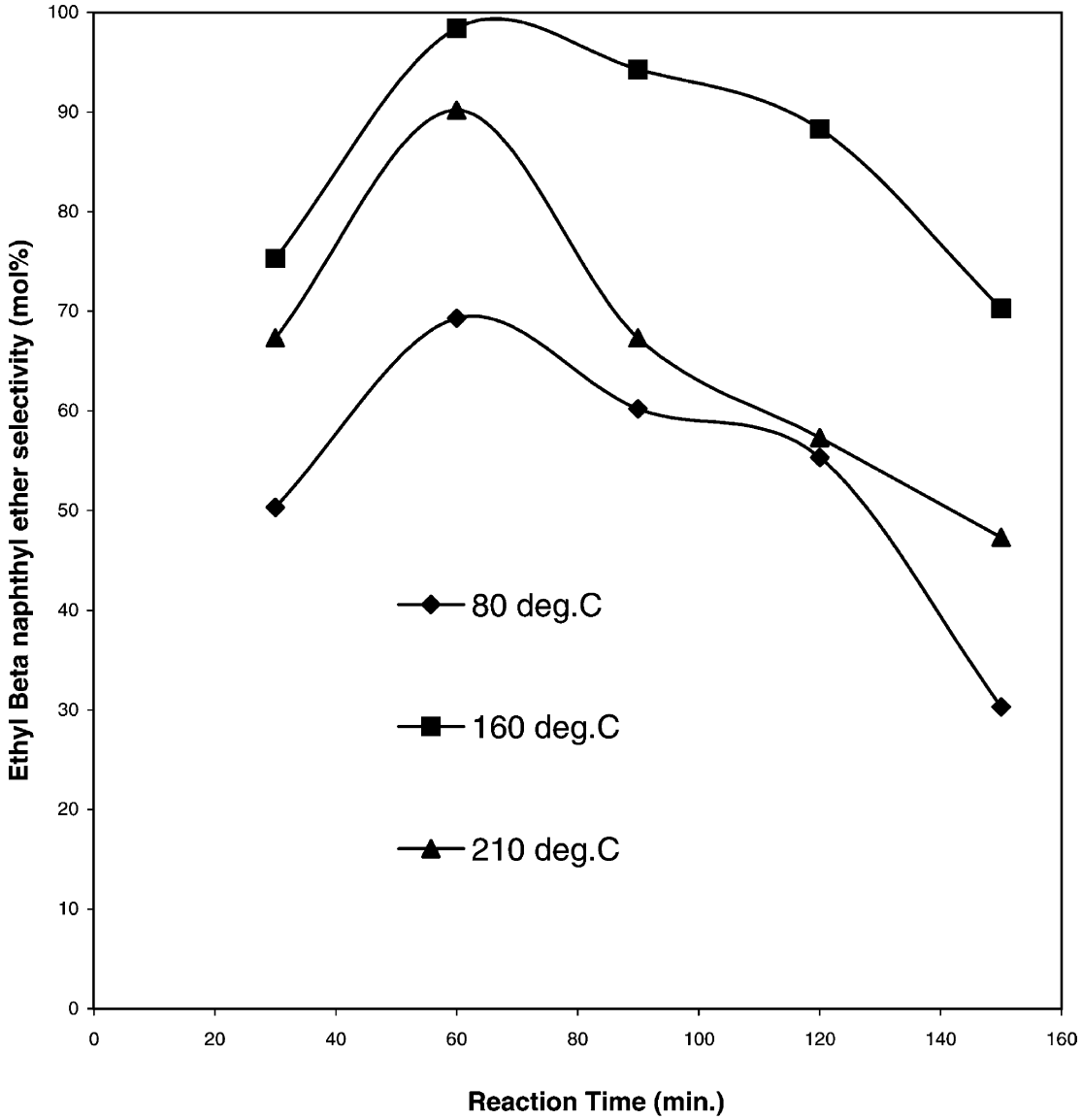

Fig. 11. Variation of ethyl β-naphthyl ether selectivity with reaction time (min).

the acid strength of H-ZSM-5 is the highest among all solid catalysts, its low catalytic activity is due to the small pore size that hinders both the entry of β-naphthol and the formation of ethyl β-naphthyl ether and the ethyl β-naphthyl ether selectivity with various catalysts was shown in the Fig. 13. Here a novel catalytic result is observed for SO_4^{2-}/Al-MCM-41 molecular sieve. When Al-MCM-41 is impregnated with 0.8 N H_2SO_4, the yield of ethyl β-naphthyl ether increases from 40.8 to 70.3 mol%, a value that is even much higher than that obtained from sulfuric acid (68.9 mol%). Therefore, sulfuric acid modification of Al-MCM-41 enhances both the catalyst activity and the catalytic acidity. To

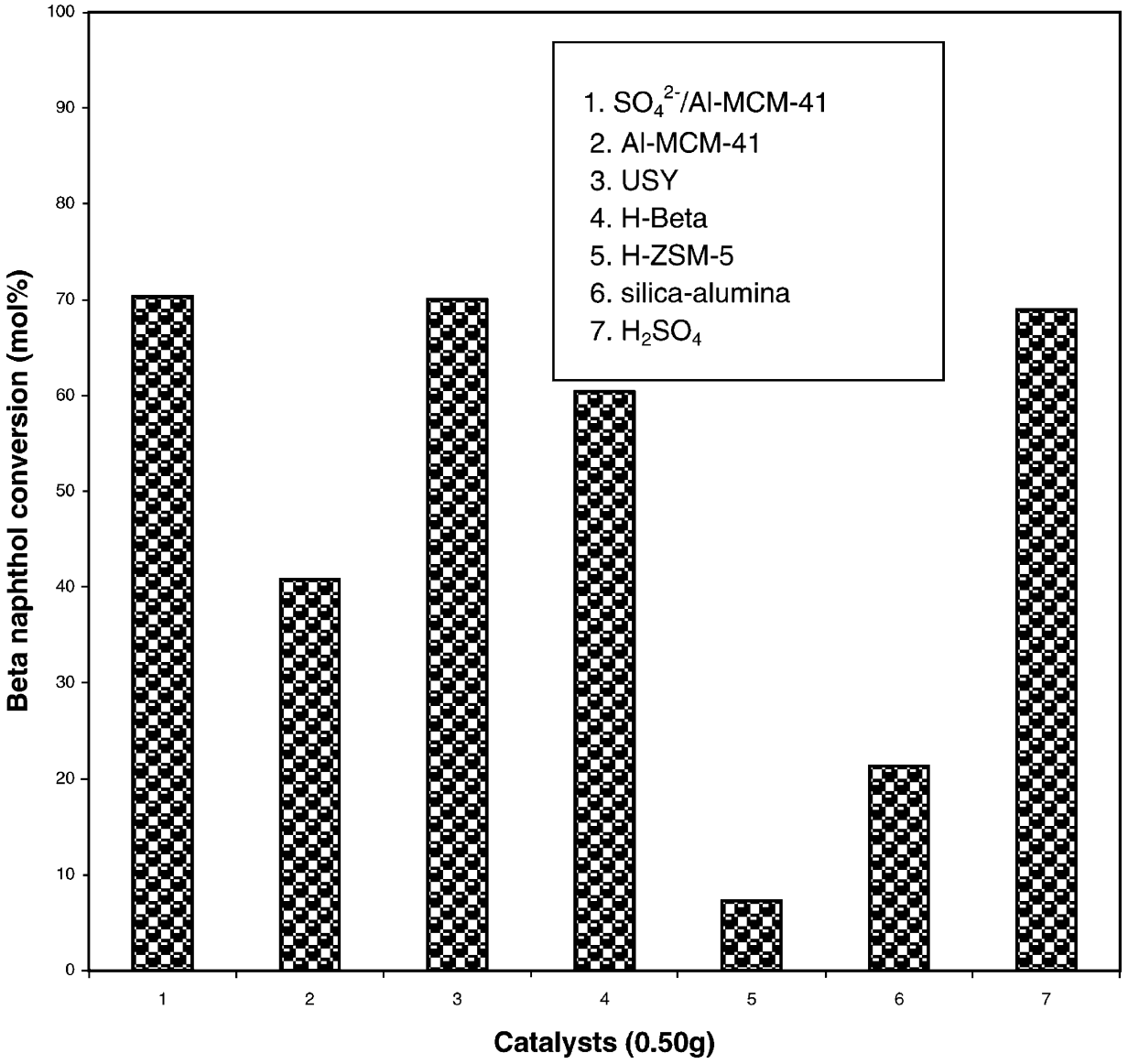

Fig. 12. Variation of conversion of β-naphthol (mol%) with various catalysts.

investigate the reasons for such a result, the sulfated Al-MCM-41 was stirred and washed with deionized water. The filtrate was found via atomic absorption spectroscopy to contain aluminum cation. Further, the resulting catalyst exhibits a significant decrease of β-naphthol conversion from 70.3 to 50.1%. Therefore, the non-framework aluminum existing in the intrachannel space is supposed to increase the catalyst activity due to the increase of Lewis acidity [26].

3.2.5. *Leaching studies of SO_4^{2-}/Al-MCM-41*

From the experiments on leaching studies carried out using SO_4^{2-} impregnated Al-MCM-41, it was observed that their was no leaching of SO_4^{2-} from the catalyst after catalytic reaction.

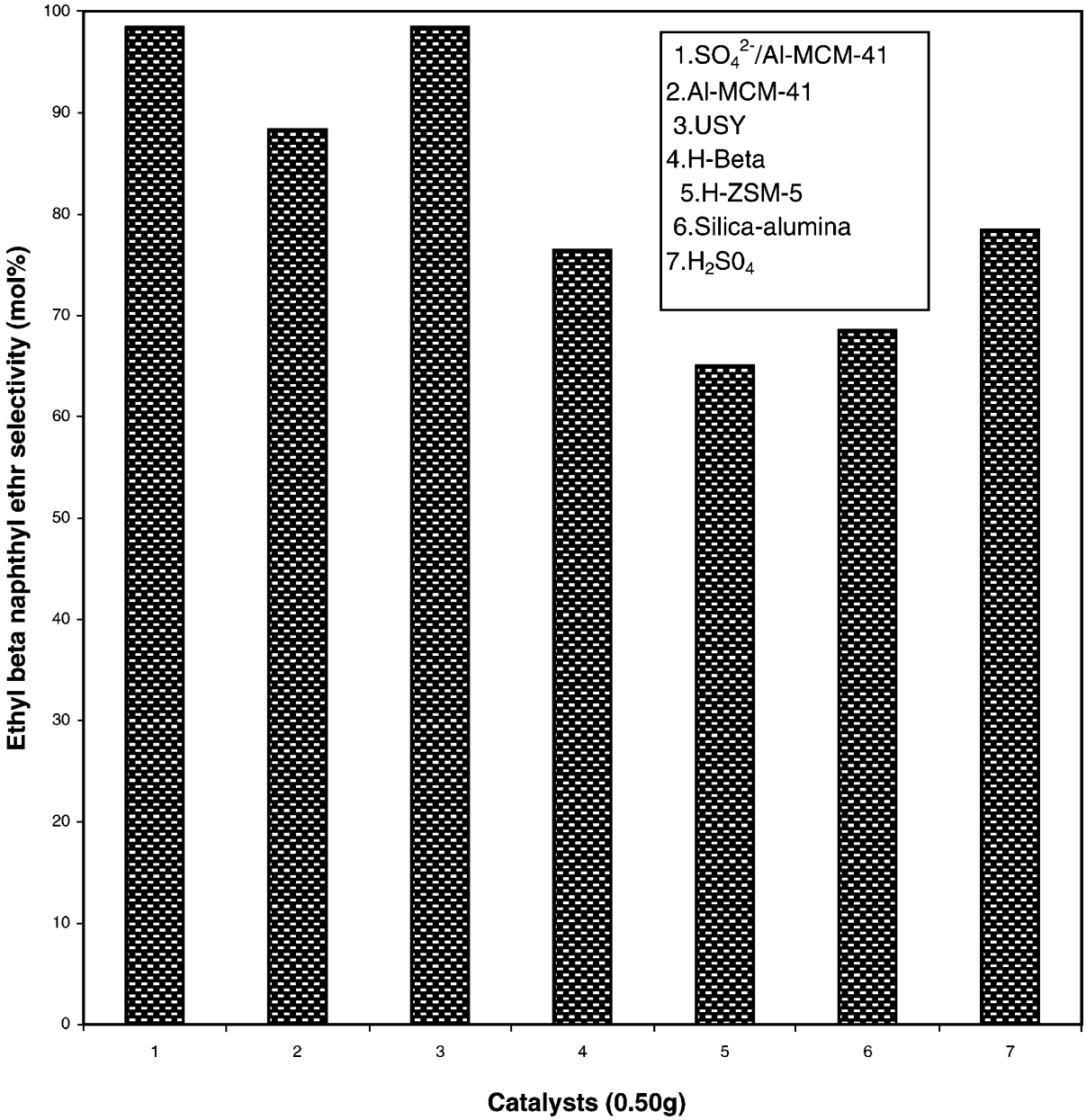

Fig. 13. Variation of ethyl β-naphthyl ether selectivity with various catalysts.

4. Conclusions

Mesoporous Al-MCM-41 was synthesized by cetyltrimethylammonium bromide under hydrothermal conditions and impregnated by sulfuric acid to get SO_4^{2-}/Al-MCM-41. The materials were characterized using XRD, N_2-adsorption, FT-IR and TG–DTA techniques. Sulfuric acid treatment of Al-MCM-41 sample results in a decease of surface area from 1099 to 698 m^2/g, pore diameter from 28.3 to 25.8 Å and

pore volume from 1.48 to 0.84 cm^3/g. The materials were evaluated for their efficiency with respect to ethoxylation of β-naphthol in the liquid phase for the production of ethyl β-naphthyl ether. The SO_4^{2-}/Al-MCM-41 catalyst forms the exclusive product of ethyl β-naphthyl ether and has much higher yields than catalysts except USY and very high selectivity of ethyl β-naphthyl ether in 10:1 molar ratio for 1 h at 160 °C. The SO_4^{2-} has been impregnated in an irreversible manner on the Al-MCM-41.

Acknowledgements

The authors express their thanks to Dr. K.S. Viswanathan, S.S. Raj, A.G. Shanmugamani, Puspha Muthiah and M. Cheralathan for their help in the characterization of the samples by FT-IR, GC, surface area techniques. The authors also thank S. Ramachandran and K. Ranganathan for their assistance in the experimental work.

References

[1] J.Y. Ying, C.P. Mehnert, M.S. Wong, Angew. Chem. Int. Ed. Engl. 38 (1992) 56.
[2] A. Corma, Chem. Rev. 97 (1997) 2373.
[3] C.T. Kresge, M.E. Leonowicz, W.J. Roth, J.C. Vartuli, J.S. Beck, Nature 359 (1992) 710.
[4] J.M. Kim, R. Ryoo, Bull. Korean Chem. Soc. 17 (1996) 66.
[5] C.Y. Chen, H.X. Li, M.E. Davis, Micropor. Mater. 2 (1993) 17.
[6] D. Das, C.M. Tasi, S. Cheng, Chem. Commun. (1999) 473.
[7] R. Ryoo, S. Jun, J. Phys. Chem. B 101 (1997) 317.
[8] R. Mokaya, J. Phys. Chem. B 103 (1999) 10204.
[9] F.D. Renzo, N. Coustel, M. Mendiboure, H. Cambon, F. Fajula, Stud. Surf. Sci. Catal. 105 (1997) 69.
[10] K. Moller, T. Bein, Chem. Mater. 10 (1998) 2950.
[11] A. Corma, V. Fornce, M.T. Navarro, J. Perez-Parients, J. Catal. 148 (1994) 569.
[12] M. Busio, J. Janchen, J.H.C. Van Hooff, Micropor. Mater. 5 (1992) 211.
[13] L.-W. Chen, C.-Y. Chou, A.-N. Ko, App. Catal. A 178 (1999) L1–L6.
[14] P. Bentev, J. Am. Chem. Soc. 74 (1952) 6118.
[15] P.T. Tanev, T.J. Pinnavaia, Science 267 (1995) 865.
[16] M.L. Occelli, S. Biz, A. Auroux, G.J. Ray, Micropor. Mesopor. Mater. 26 (1998) 193.
[17] J.S. Beck, J.C. Vartuli, W.J. Roth, M.E. Lernowicz, C.T. Kresge, K.D. Schmitt, C.T.W. Chu, D.H. Olson, E.W. Sheppard, S.B. Mccullen, J.B. Higgins, J.C. Schlenker, J. Am. Chem. Soc. 144 (1992) 10834.
[18] J.-H. Kin, M. Tanabe, M. Niwa, Micropor. Mater. 10 (1997) 85.
[19] S.J. Gregg, K.S.W. Sing, Adsorption, Surface Area and Porosity, 2nd ed., Academic Press, New York, 1982.
[20] T.R. Pauly, Y. Liu, T.J. Pinnavaia, S.J.L. Billinge, P. Rieler, J. Am. Chem. Soc. 121 (1992) 8835.
[21] J.R. Sohn, S.J. Decanio, J.H. Lunsford, D. Odennell, Zeolites 3 (1986) 225.
[22] A.V. Kiseler, V.I. Lygin, Infrared Spectra of Surface Compounds and Adsorbed Substances, Nauka, Moskow, 1992 (in Russian).
[23] M.A. Cambler, A. Corma, J. Pereg-Pariente, J. Chem. Soc., Chem. Commun. (1993) 147.
[24] C.N. Rao, Chemical Application of Infrared Spectroscopy, Academic Press, New York, 1963, p. 339.
[25] J. Medina-Valtieera, O. Zaldivar, M.A. Sanchez, J.A. Montoya, J. Navarrete, J.A. de los Reyes, Appl. Catal. A 166 (1998) 387.
[26] J. Medina-Valtieera, M.A. Sanchez, J.A. Montoya, J. Navarrete, J.A. de los Reyes, Appl. Catal. A 158 (1997) L1.